ELSEVIER
Nuclear Instruments and Methods in Physics Research A 444 (2000) 228–231
NUCLEAR INSTRUMENTS & METHODS IN PHYSICS RESEARCH Section A
www.elsevier.nl/locate/nima

Single-photon 2-D imaging X-ray spectrometer employing trapping with four tunnel junctions

L. Li[a], L. Frunzio[a], K. Segall[a], C.M. Wilson[a], D.E. Prober[a,*], A.E. Szymkowiak[b], S.H. Moseley[b]

[a]*Department of Applied Physics, Yale University, New Haven, CT 06520, USA*
[b]*NASA Goddard Space Flight Center, MD 20771, USA*

Abstract

We are developing single-photon 2-D imaging X-ray spectrometers for applications in X-ray astrophysics. The devices employing a Ta strip X-ray absorber with Al traps and a tunnel junction at each end have been tested. They achieve an energy resolution of 26 eV out of 5.9 keV over a limited length (Segall, IEEE Trans., in press) with a 1-D spatial resolution of about 2 μm over the full 160 μm length. By analytical and numerical simulations of the quasiparticle diffusion process, we study related devices with a square Ta absorber having four traps and attached junctions to provide 2-D imaging. The traps give charge division to the corners or to the edges of the square absorber. We find that these devices can give good 2-D spatial resolution. We discuss the operating principle and the factors which affect the spatial resolution.

1. Introduction

Superconducting tunnel junctions have been extensively used in developing single-photon X-ray spectrometers. In the last 10 years, they have been integrated in different devices which also performed imaging. We have developed a single-photon imaging X-ray spectrometer employing lateral trapping in order to detect photons with competitive energy and spatial resolutions. These devices employ a Ta strip absorber with Al traps. The energy of a photon absorbed in a superconductor can break Cooper pairs and excite quasiparticles. The number of quasiparticles created is proportional to the energy of the photon. The quasiparticles diffuse in the absorber and are collected in the traps. They tunnel through each junction. When an X-ray is absorbed at time $t = 0$ at position $x = x_0$, $y = y_0$, the dynamics of the quasiparticle distribution $n(x, y, t)$ inside the absorber can be described by a standard diffusion equation including a term for quasiparticle loss on a time scale of τ_{loss} to account for the finite life time. Since the process of quasiparticle generation is fast on the time scale of the diffusion inside the absorber, the initial distribution can be assumed to be point-like. Quasiparticles at the absorber-trap interfaces will be trapped into each trap by inelastic scattering. The resulting differential equation is

$$\frac{\partial n(x, y, z)}{\partial t} = D\nabla^2 n(x, y, t) - \frac{n(x, y, z)}{\tau_{\mathrm{loss}}}.$$

* Corresponding author.
E-mail address: daniel.prober@yale.edu (D.E. Prober).

0168-9002/00/$ - see front matter
PII: S0168-9002(99)01364-9

The initial condition is

$$n(x, y, 0) = N_0 \delta(x - x_0, y - y_0)$$

where D is the diffusion constant and N_0 is the total number of charges generated by the X-ray photon. We report a study performed by analytical and numerical simulations on two different designs of 2-D imaging four junction detectors shown in Fig. 1. The first device has a junction on each side and the second one has a junction on each corner. Their performance is discussed in the next section.

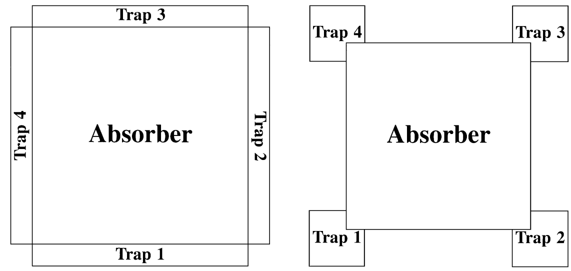

Fig. 1. The left design is an absorber with a junction at each side. The right design is an absorber with a junction at each corner.

2. Analysis

2.1. Junction on each of the four sides

In the devices we studied the trapping is close to be perfect, so it is realistic to choose perfect boundary condition as [1]

$$n|_{x=0,\ x=L} = 0, n|_{y=0,\ y=L} = 0$$

where L is the length of the absorber.

The charge collected at trap 1 Q_1 is calculated analytically and we find

$$Q_1(x, y) = \frac{4}{\pi} Q_0 \sum_{m=1}^{\infty} \frac{\sin((2m-1)(\pi x/L))}{2m-1} \times \frac{\sinh(\sqrt{(2m-1)^2 + (L^2/\pi^2 D\tau_{\text{loss}})}\,(1-(y/L))\pi)}{\sinh(\sqrt{(2m-1)^2 + (L^2/\pi^2 D\tau_{\text{loss}})}\pi)}$$

where $Q_0 = eN_0$ is the total charge produced. Charges at other traps Q_i, $(i = 2, 3, 4)$ are calculated similarly.

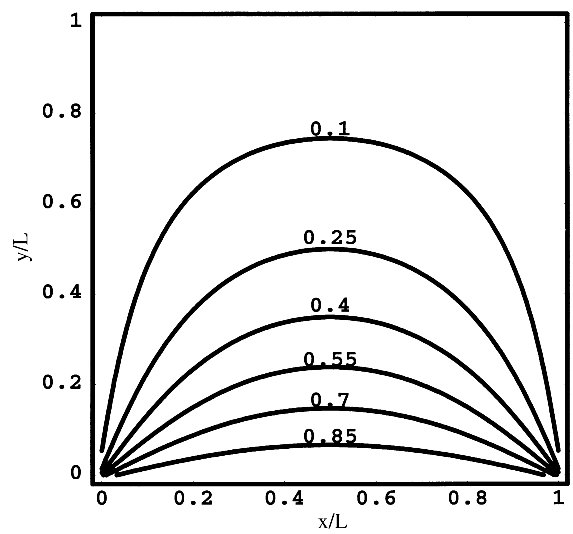

Fig. 2. Contour plot of the fraction of total quasiparticle charge Q_1/Q_0 collected in trap 1 as a function of the position of X-ray events. We assume there is no loss in the absorber and perfect trapping.

Fig. 2 shows the contour plot of the fraction of the total charge versus position of the X-ray events. If the X-ray event is close to one junction, most of the charge will be collected by that junction. The farther the photon absorption event is from the junction, the fewer quasiparticles can be collected by that junction. The bending of the equal collection lines shows the effect of the two traps close to the trap we selected. They act as trapping sinks strongly reducing the collection power of the selected junction. This behavior will be the same for all the junctions of the device. The charge collected at each of the four junctions give the information to determine both the photon energy and the position of the X-ray absorption event, which can be used to implement 2-D imaging. In order to get the best spatial resolution, we introduce combination variables $f = Q_1/(Q_1 + Q_3)$ and $g = Q_2/(Q_2 + Q_4)$. If ΔQ_i is the RMS charge noise of junction i, $(i = 1, 2, 3, 4)$, from the $\Delta Q_i/Q_0$ at each junction, the spatial resolution can be calculated.

We define

$$a_{11}(x,y) = \frac{\partial f(x,y)}{\partial x},\ a_{12}(x,y) = \frac{\partial f(x,y)}{\partial y},$$

$$a_{21}(x,y) = \frac{\partial g(x,y)}{\partial x},\ a_{22}(x,y) = \frac{\partial g(x,y)}{\partial y}.$$

Assume that the noise of the charge readout from the four junctions is not correlated and equal to ΔQ. Then

$$\sqrt{\overline{(\Delta x_i)^2}} = \frac{\Delta Q}{|a_{11}a_{22} - a_{21}a_{12}|} \times \left(\frac{a_{2i}^2}{(Q_1 + Q_3)^4}(Q_1^2 + Q_3^2) + \frac{a_{1i}^2}{(Q_2 + Q_4)^4}(Q_2^2 + Q_4^2) \right)^{1/2}$$

where $i = 1, 2$, $\Delta x_1 = \Delta y$, and $\Delta x_2 = \Delta x$.

Fig. 3 shows the normalized spatial resolution $\Delta r/L = \sqrt{(\Delta x)^2 + (\Delta y)^2}/L$ depending on position of the photon absorption, with loss and without loss in an absorber of 1 mm × 1 mm size. We assume $\Delta Q_i/Q_0 = 0.01$ and for the case of loss $D = 8\ \mathrm{cm}^2/\mathrm{s}$ [2] and $\tau_{\mathrm{loss}} = 450\ \mu\mathrm{s}$, as derived from the recent two-junction device measurements [3]. From the plot the spatial resolution in the center is better than the region near the edges. That is because when the event is close to one junction, the charge collected by the other junctions is small. The signal-to-noise ratio is thus lower, and this degrades the spatial resolution. On the contrary the spatial resolution near the center is better than 2%. Comparing the spatial resolution with and without loss, the spatial resolution is worse with loss, as expected. This can be seen in Fig. 3. For astronomy application we need a larger absorber. The improved quality of the absorber film will increase the loss time and the diffusion constant.

2.2. Junction at each of the four corners

The boundary condition changes to $n = 0$ at the four corners, quasiparticles are reflected at the other parts of the boundary. The corner traps extend over 10% of each side.

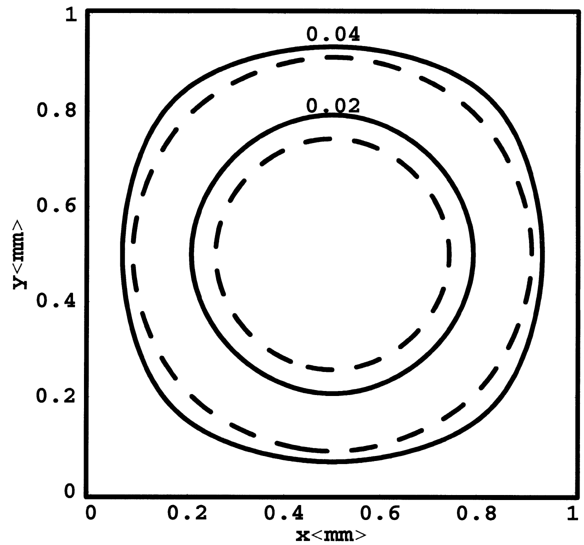

Fig. 3. Contour plot of the spatial resolution $\Delta r/1$ mm of a 1 mm × 1 mm absorber with junctions on four sides. The solid contour line is the spatial resolution with no charge loss. The dashed contour line is the spatial resolution with charge loss. For each junction we assume that each readout has charge noise of $\Delta Q_i/Q_0 = 0.01$.

In this case, due to the complexity of the problem, the random walk method [4] has been used to solve for the charge collected at each of the four corners as a function of the location of absorption in the absorber. Fig. 4 shows the results of the fractional charge collected in one junction without loss.

Similar to the method for the previous device, the same variables f and g are defined to determine the location of the X-ray absorption event. Fig. 5 shows the spatial resolution normalized to the absorber size of the detector with the junctions at four corners.

Comparing the two designs, the device with the junctions at the four corners gives almost the same spatial resolution as the device with the junctions at four sides. In fact, in spite of the better spatial separation of charge in the four-corner junction device, we lose information about the charge position near the center of the edges due to random reflection of the quasiparticles at the boundary with no traps. This device with junctions at four corners is more sensitive to the loss of quasiparticles

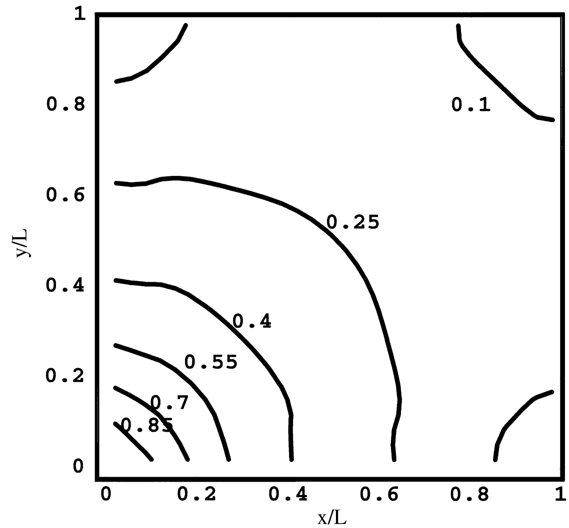

Fig. 4. Contour plot of the fraction of the total quasiparticle charge Q_1/Q_0 collected in trap 1 as a function of the position of X-ray absorption events. We assume there is no loss in the absorber and perfect trapping.

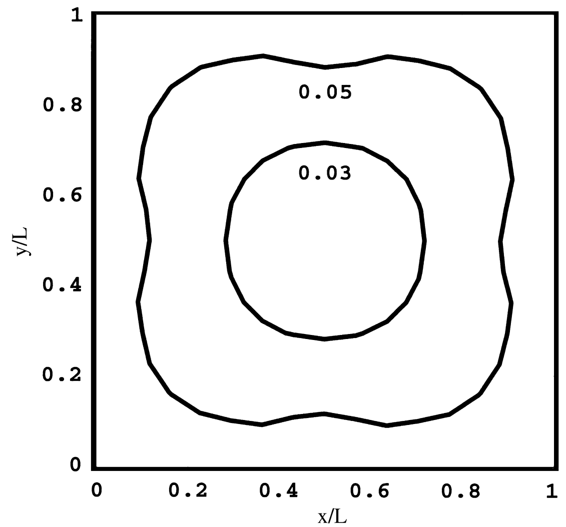

Fig. 5. Contour plot of the spatial resolution $\Delta r/L$ normalized to the absorber size with junctions at four corners. For each junction we assume that each readout channel has charge noise of $\Delta Q_i/Q_0 = 0.01$.

because its junctions take a longer time to collect the quasiparticles generated by X-ray photons.

3. Conclusion

We have studied two designs of four junction devices. Our results show that they can provide good 2-D imaging. The loss of quasiparticles in the absorber affects the spatial resolution of the device. With the life time we measured in a recent two-junction device, the 1mm × 1mm absorber still can provide very good spatial resolution. The advantage of such 4-junction devices compared to arrays of single pixels [5,6] is that one can implement 2-D maging with only four readout channels, with effectively 10^3 or more pixels.

References

[1] H. Kraus et al., Phys. Lett. B 231 (1989) 195.
[2] S. Friedrich et al., Appl. Phys. Lett. 71 (1997) 3901.
[3] K. Segall et al., Energy Resolution of Imaging X-Ray Spectrometers, Low Temperature Detectors LTD8 poster.
[4] J. Tobochnik, Comput. Phys. 4 (1990) 181.
[5] N. Rando et al., Soft X-ray response of a 36 pixels superconducting tunnel junction array for high-resolution X-ray astronomy, Proceedings of the SPIE 3445, 1998, paper no. 25.
[6] J.A. Chervanek et al., Appl. Phys. Lett. 74 (1999) 4043.